Influence of MoO₃ on the Structure of Lithium Aluminum Phosphate Glasses

Yasser B. SADDEEK[(1)], S. M. ABO-NAF[(2)]

[(1)] *Physics Department, Faculty of Science, Al-Azhar University*
Assiut 71524, Egypt; e-mail: ysaddeek@gmail.com

[(2)] *Glass Research Department, National Research Centre (NRC)*
El-Behoos Str., Dokki, 12622 Cairo, Egypt

IR spectroscopy, density and ultrasonic velocity measurements have been carried out for aluminum lithium phosphate glasses with and without MoO₃. The observed changes in the FTIR spectra of the glasses were related to the modifier/former role of molybdenum ions. The results revealed that the density increases with increasing MoO₃ content, which was attributed to the increase in the compactness and packing of the glass network. The ultrasonic data were analyzed in terms of creation of new bonds of MoO₃ attached to phosphate units. The new bonds increased the average crosslink density and the number of network bonds per unit volume along with a strengthening of the different modes of vibrations which in its turn increased the ultrasonic velocity, the rigidity and hence the elastic moduli of the glasses.

Keywords: phosphate glasses, IR, density, elastic properties.
PACS: 43.35.Ae, 61.43.Fs, 62.20.Dc, 62.80.f, 78.30.Ly, S10.15.

1. Introduction

Lithium phosphate glasses have been gained great attention during the last decades due to their wide range of compositional and structural possibilities. The low melting and glass transition temperatures, high electrical conductivity, high thermal expansion coefficient of these glasses enable their use in laser host matrices, lithium micro-batteries or in electro-optical systems (Chowdari, 1988; Selvaraj, 1988; Chowdari, 1991; Donald, 1993; Proulx, 1994; Jiang, 1998; Hudgens, 1998; Brow, 2000; Campbell, 2000; Dai, 2002; Sharaf El-Deen, 2008; Cozar *et al.*, 2008). The physical properties of phosphate glasses can be improved by introducing alumina, which provides higher chemical durability, alkali and transition metal oxides like MoO₃ (Bridge *et al.*, 1986; 1987; Chen, 1999; Reis *et al.*, 2002).

It was reported that the network of lithium phosphate glasses is a polymeric arrangement of phosphate groups with variable lengths, and is dominated by linkages between PO₄ tetrahedra. Addition of Li₂O to P₂O₅ converts the three-dimensional phosphate network into linear phosphate chains, and changes the phosphate structural groups from PO₄ to PO₃ to PO₂ to PO as the molar ratio of Li₂O/P₂O₅ passes from 0 to 1, to 2 and to 3. The linear chain structure results in a cleavage of P–O–P linkages and a creation of non-bridging oxygens (NBO's) in the glass (Wells, 1975; Rao, 2002; Prasad, 2005; ElBatal *et al.*, 2008; Šubčik *et al.*, 2009). On the other hand, the structure of MoO₃-P₂O₅ glasses were stated to belong to a group of glasses, which incorporate distorted octahedral structural units [MoO₆] or tetrahedral structural units [MoO₄] within the glass network. MoO₃ plays a modifier role upon the addition of MoO₃ to P₂O₅ glasses with ratio <50 mol% by forming non-bridging oxygens, and a former role when MoO₃ > 50 mol% throughout the complete Mo-P-O range by increasing the crosslink density of P₂O₅ (Bridge *et al.*, 1986; 1987; Moustafa *et al.*, 1998).

Introducing molybdenum ions in lithium phosphate glasses produces some variable interesting electrical properties which are related to the ability of molybdenum ions to exist in glasses in three possible valences, namely Mo³⁺, Mo⁵⁺ and Mo⁶⁺ (Bih *et al.*, 2008; ElBatal *et al.*, 2008; Chowdari *et al.*, 1991). Recently, it was found that substitution of PbO by MoO₃ in MoO₃–PbO-La₂O₃–P₂O₅ glasses leads to a polymerization of the phosphate chains by increasing the packing and the cross link density of the phosphate network (Saddeek, 2011). Accordingly, this work aims

to extend the available informations of MoO_3 in the environment of the Al_2O_3-P_2O_5-Li_2O glass system by using FTIR and ultrasonics to study its availability for the use in opto-electronic devices in a further work.

2. Experimental procedures

Glass samples with the formula x MoO_3-$2Al_2O_3$-$68P_2O_5$-$30Li_2O$ with $0 \leq x < 40$ wt% were prepared by the melt-quenching technique. The starting materials to obtain these glasses are $(NH_4)_2HPO_4$, Li_2O, Al_2O_3 and MoO_3 of reagent grade purity. The starting materials were mixed together by grinding the mixture repeatedly to obtain a fine powder. The mixture was melted in a porcelain crucible in an electrically heated furnace under ordinary atmospheric conditions at a temperature of about 1273 K for 2 h to homogenize the melt. The obtained glass samples from the melt quenching into preheated stainless-steel mould were heat treated at a temperature of about 20K below their calorimetric glass transition temperature for 2 h to remove any internal stresses. The obtained glasses were lapped and two opposite sides were polished to be suitable for use in the ultrasonic velocity measurements. Non-parallelism of the two opposite side faces was less than $0.01°$. The composition given in table 1 refers to the nominal composition (the starting mixture). The glass samples were kept in desiccators to prevent possible attack by moisture. X-ray diffraction patterns were recorded to check the amorphous nature of the glass samples using a Philips X-ray diffractometer PW/1710 with Ni-filtered Cu-K_α radiation ($\lambda = 1.542$ Å) powered at 40 kV and 30 mA. The patterns (not shown) revealed broad humps characteristic of the amorphous materials and did not reveal discrete or any sharp peaks.

Infrared (IR) spectra for the glass powder (after crushing them into powder form) were obtained using an IR Fourier spectrophotometer type JASCO, FT/IR–430 (Japan). For this purpose, each sample was mixed with KBr in the proportion of $1:100$ (by weight) for 20 min and pressed into a pellet using a hand press. At least two spectra for each sample were recorded in the wavenumber range of 400–2000 cm^{-1} with a resolution of 4 cm^{-1}, corrected for dark-current noise and normalized. The resulted spectra were curving fitted (PROULX *et al.*, 1994) to get quantitative values for the band areas of heavily overlapped bands. The curve-fitting procedure is based on a least-squares minimization which in its turn involves entering the values of the wavenumber of the component bands (determined by using the deconvolution technique) and then a program determines the best estimate of the parameters of the component curves. The deconvolution process involves several steps: computation of an interferogram of the sample by computing the inverse Fourier-transform of the spectrum, multiplication of the interferogram by a smoothing function and by a function consisting of a Gaussian–Lorentzian band shape and Fourier transformation of the modified interferogram. The deconvolution procedure is typically repeated iteratively for best results. At iteration, the line shape is adjusted in an attempt to provide narrower bands without excessive distortion. Therefore, each IR spectrum has its characteristic peak positions.

The density ρ of the glass samples was determined using the Archimedes technique by applying toluene as an immersion fluid. At least, three samples of each glass were used to determine the density. A random error in the density values was found as $\pm 1\%$. The molar volume V_m has been determined as M/D, where M is the molar weight of the glass. The values of the packing density (V_t) were calculated as $V_t = (1/V_m) \sum_i V_i x_i$, where $V_i = (4\pi/3)N_A[mR_A^3 + nR_O^3]$, R_A and R_O are the Pauling radii (Å) of ions in the oxide A_mO_n.

The ultrasonic velocities, longitudinal (ν_L) and shear ones (ν_T), at room temperature ($\sim$300 K) were obtained using the pulse-echo method. In this method, x-cut and y-cut transducers (KARL DEUTSCH) operated at the fundamental frequency of 4 MHz along with a digital ultrasonic flaw detector (KARL DEUTSCH Echograph model 1085) were used. The uncertainty in the measurement of the ultrasonic velocity is ± 10 m/s. Besides the density, two velocities were utilized to determine two independent second-order elastic constants (SOECs): C_{11} and C_{44}. For the pure longitudinal waves $C_{11} = \rho v_L^2$, and for the pure transverse ones $C_{44} = \rho v_T^2$. The bulk modulus (K_e), Young's modulus (Y), the Debye temperature (θ_D) and the Poisson's ratio (σ) may be determined using the standard relations (RAO, 2002):

$$\sigma = 1/2 - C_{44}/2(C_{11} - C_{44}), \qquad (1)$$

$$Y = 2(1 + \sigma)C_{44}, \qquad (2)$$

$$K_e = C_{11} - 4/3C_{44}, \qquad (3)$$

$$\theta_D = (h/k)v_D \left[\frac{3q\,\rho\,N_A}{4\pi\,M}\right]^{1/3}, \qquad (4)$$

where v_D is the mean ultrasonic velocity given by $\left[\frac{1}{3}\left(\frac{1}{v_L^3} + \frac{2}{v_T^3}\right)\right]^{-1/3}$, h is the Planck's constant, N_A is the Avogadro's number, and k is the Boltzmann's constant. The uncertainty in the measurement of the elastic moduli is ± 0.15 GPa.

3. Results and discussion

3.1. Structural analysis

Figure 1 shows the IR spectra of the Al_2O–Li_2O-P_2O_5 glass system with and without MoO_3 Figures 2 a–c show the deconvolution of the IR spectrum of the glasses containing different ratios of MoO_3 wt% as an

example. The main features of the IR spectra of the studied glasses are four bands at ∼525, ∼745, ∼1088 and ∼1645 cm^{-1}. The presence of MoO_3 creates two additional bands at ∼1268 and ∼1430 cm^{-1}. The common IR features of these glasses are that the absorption bands for glasses containing MoO_3 become wider, and their broadening increases with the increasing MoO_3 content. Moreover, the absorption bands are strongly overlapped especially at ∼525 and ∼1000 cm^{-1}. The position of the absorption band at ∼745 cm^{-1} was shifted to a lower wavenumber and its area became decreased. Moreover, the absorption band at 1000 cm^{-1} was shifted to a higher wavenumber.
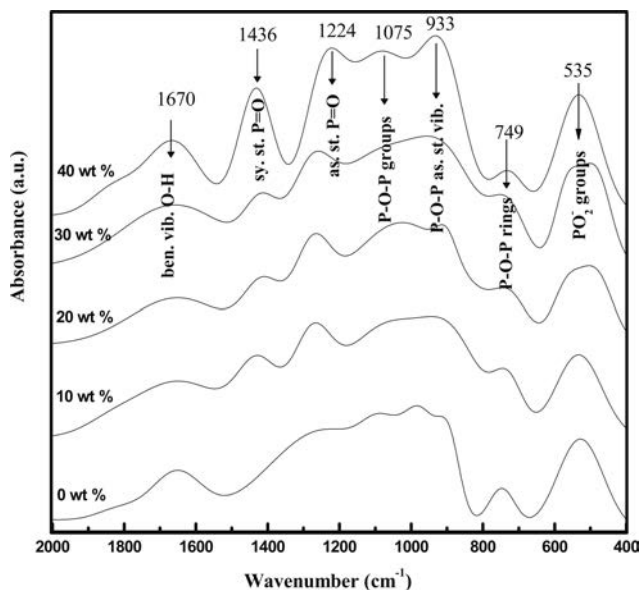

Fig. 1. Infrared absorption spectra of the glass system $2Al_2O_3$-$30Li_2O$-$68P_2O_5$-$x$$MoO_3$ ($0 \leq x \leq 40$ wt%).

The IR absorption at around 520 cm^{-1} is attributed to the bending vibrations of the O=P–O linkages (Ciceo Lucacel *et al.*, 2009). This band may be superimposed with the vibrations of the MoO_6 structural units that play a modifier role (Little Flower *et al.*, 2007). The bands at around 745 cm^{-1} are assigned to asymmetric stretching vibrations of the P–O–P rings (Moustafa *et al.*, 1998) The bands at around 910 cm^{-1} are related to P–O–P symmetric stretching vibrations of bridging oxygen atoms in the P–O–P bonds (Sudarsan *et al.*, 2004). The band at around 995 cm^{-1} can be ascribed to symmetric stretching vibration of the PO_4^{3-} tetrahedra (P–O$^-$ ionic group) (Jastrzebski *et al.*, 2011; Lazarev, 1968; Ciceo Lucacel *et al.*, 2009) This band may be overlapped with another one ascribed to the Mo-O stretching vibration in the $[MoO_4]^{2-}$ units that play a former role (Šubčik *et al.*, 2009). The vibrational bands at around 1275 and 1410 cm^{-1} have been attributed to the asymmetric stretching of the double bonded oxygen vibrations and to the symmetric stretching mode of P=O (Sudarsan,
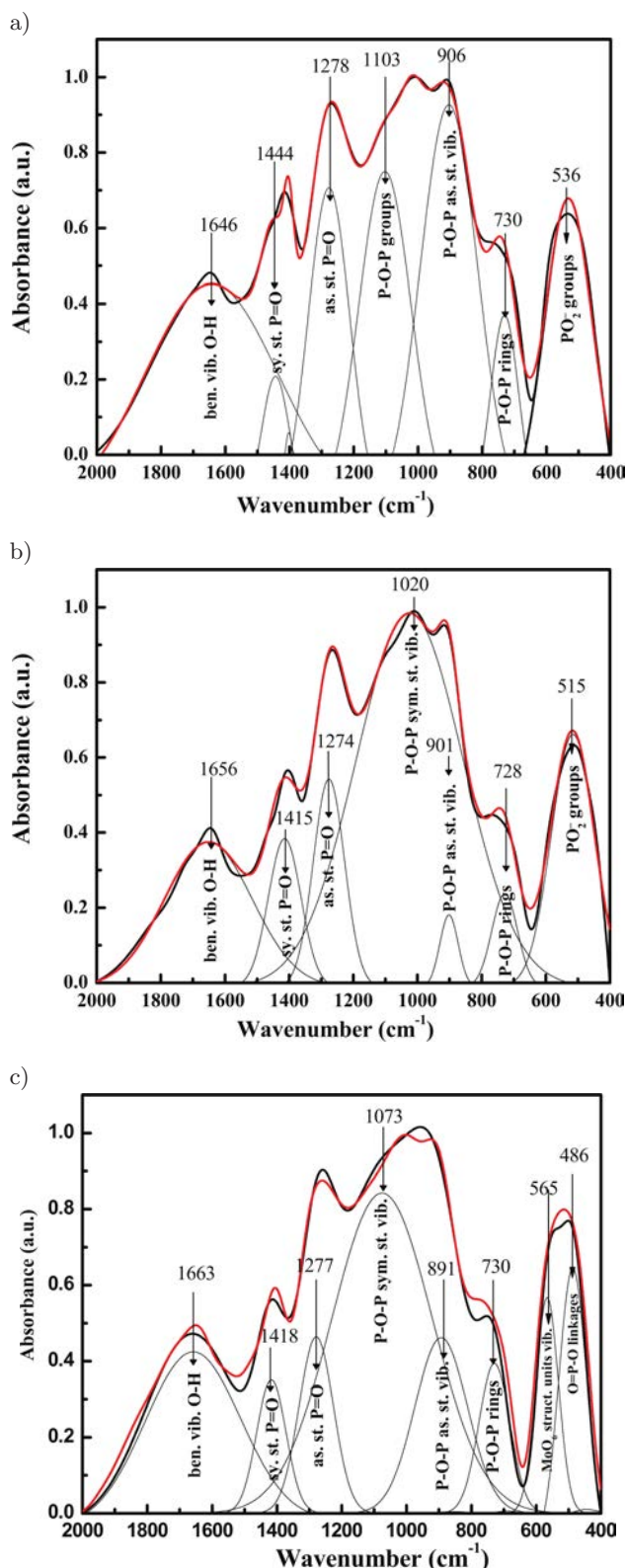

Fig. 2. Band deconvolution of the IR spectrum for $2Al_2O_3$-$30Li_2O$-$68P_2O_5$-$x$$MoO_3$ glass ($0 \leq x \leq 40$ wt%; a) $x = 10$, b) $x = 20$, c) $x = 30$

2004; Magdas *et al.*, 2008) In addition to the above features, there is a small absorption band in the spectra of all glasses at around 1660 cm^{-1}. Such a band

was attributed to the bending vibrations of O-H bonds brought by air moisture during the preparation of the KBr pellets for the infrared measurements (KHAFAGY, 2001; BOUDLICH *et al.*, 2002).

Recently, it was reported that in Li_2O-P_2O_5 glasses, the increase of the Li_2O content causes the formation of terminal phosphate groups PO_3^{2-} and an increase in the average length of the P=O bond (IVASCU *et al.*, 2011). An addition of Al_2O_3 to lithium phosphate glasses causes a shift of the main absorption bands of the PO_4 units to higher wavenumbers. This shift was attributed to two reasons; the first one is the formation of P–O–Al bridging bonds connected to phosphate groups instead of P–O–Li bonds where Al–O has a higher bond strength than P-O; the second one is the formation of charge compensation pairs between Li^+ and the aluminum (VI) polyhedra (BROW, 2000; MANUPRIYA, 2009; LIDE, 2004). Therefore, as represented in the studied glass system, as the MoO_3 content is increased, for $0 \leq x \leq 20$ and $20 \leq x \leq 40$ (wt%) two regions can be formed in the IR spectra as shown in Fig. 1. The features of the first region are,

a) the intensity of the vibrational bands related to the phosphate glasses is decreased,

b) the bands due to symmetric stretching vibrations of P–O–P rings are shifted to a lower wavenumber,

c) the bands due to P–O–P asymmetric stretching vibrations of the bridging oxygen atoms in the P–O–P bonds are rapidly shifted to a higher wavenumber.

These features suggest the modifier role of MoO_3 by breaking up the P–O–P linkages and occupying the positions between P–O–P layers creating NBOs to form MoO_6 without a change of the number of P=O bonds the features of the second regions are:

a) the intensity of the illustrated vibrational bands related to phosphate glasses is increased,

b) the whole of the latter bands are shifted to a higher wavenumber.

The shift of the bands can be explained by taking into account the strength of the bands and the effect of the bond energy of Mo-O. The strength of the vibrational bands can be attributed to the decrease in the phosphate chains length, the increasing ratio of the oxygen atoms to the phosphorus ones (O/P), and to the bridging of Mo with oxygen atoms to form $[MoO_4]^{2-}$ units which have a former role. In this region, MoO_3 enters the glass network by breaking up the P–O–P linkages and forming P–O–Mo bonds. Accordingly, the P=O bond will be converted into bridging oxygen and the phosphate bonds will be shortened (HIGAZY, 1985; COZAR *et al.*, 2006). The overlapping of the absorption bands in this region confirmed the formation of shorter bonds, and the value of O/P larger than 3 confirmed the rupture of P=O bonds. A similar behavior in tungsten lead phosphate glasses has been observed (ABID *et al.*, 2002).

3.2. Analysis of the elastic moduli

Table 1 shows the values of the density of MoO_3-Li_2O-Al_2O_3-P_2O_5 glasses with the different additions of MoO_3. The values of the density of the studied glasses agree well with that reported elsewhere (Abid, 2002; Montenero, 2004; Cozar et al., 2006). In general, both the packing of the glass network and the molecular weight of each contributed oxide affect the density in the glass system. It is generally accepted that the density increases when the concentration of the third component (MoO_3) is increased while the ratio of the other concentrations remain always constant.

On the other hand, the packing density of Li_2O, Al_2O_3, P_2O_5 and MoO_3 are considered to be 8, 21.5, 34.8 and 21.3 $m^3 mol^{-1}$, respectively (WELLS, 1975; SADDEEK, 2011). Accordingly, the Mo^{3+} ions can occupy an interstitial position in the interstices of the lithium phosphate network increasing the connectivity of the structure with further addition of the MoO_3 content. Thus, the increase in the density can be related to the constitution of the glasses rather than to the type of the structural unit.

As reported earlier, the ultrasonic velocity into a glassy material depends on the rigidity, cross-link density and the number of bonds per unit volume of the structure of the glasses, i.e. a harder material will produce a higher velocity, whereas a softer material will produce lower velocity, irrespective of their densities (BRIDGE, 1986; SADDEEK, 2007; ERAIAH *et al.*, 2010). The variation of the values of the longitudinal and shear ultrasonic wave velocities with the MoO_3 content is listed in Table 1. The ultrasonic velocities, Debye temperature (θ_D), and the elastic moduli, i.e. the Young's modulus (Y) and bulk modulus (K_e) of the studied glasses, increase while the Poisson's ratio decreases with the increase of the MoO_3 content.

According to the IR analysis, there is some type of modification of the chemical bonds linked to the phosphate structural units with the addition of MoO_3 in the interstices of the lithium phosphate network This addition creates $[MoO_4]^{2-}$ structural units bridging oxygens and smaller rings of the phosphate groups. This creation is associated with an increase of O/P and bridging bonds P-O-Mo that has high bond energy. These factors contribute to the increase of the average crosslink density (n_c) and to the number of network bonds per unit volume (n_b) of the glass system. The average crosslink density and the number of network bonds per unit volume can be estimated according to an earlier work (Higazy et al., 1985). Thus, the observed increase in the ultrasonic velocity can be explained by assuming that, Mo^{3+} enter interstitially and as a result some type of modification of the P–O–P, and Li–O–P linkages, which already exist in the glass, into Mo–O–P, and Li–O–P bonds will occur. The conversion of these linkages results in an increase in

Table 1. The density (ρ), packing density (V_t), longitudinal (v_L) and shear (v_T) ultrasonic velocities, Debye temperature (θ_D), Poisson's ratio (σ), average cross link density (n_c), number of network bonds per unit formula unit (n_b), Young's modulus (Y), and the bulk modulus (K_e) of the glass system $2Al_2O_3$-$30Li_2O$-$68P_2O_5$-$xMoO_3$ glass (where $x = 0, 10, 20, 30$ and 40 wt%).

Composition of glass wt%				ρ	V_t	v_L	v_T	θ_D	σ	n_c	$n_b \times 10^{28}$	Y	K_e
Li_2O	Al_2O_3	P_2O_5	MoO_3	[kg/m³]	–	[m/s]	[m/s]	[K]	–	–	[m³]	[GPa]	[GPa]
30	2	68	0	3566	0.60	4103	2210	332.2	0.217	2.84	7.11	68.6	35.44
30	2	68	10	3644	0.62	4155.8	2245	341	0.215	2.90	7.31	69.7	35.98
30	2	68	20	3717	0.64	4202	2278	348.7	0.212	2.97	7.54	70.7	36.60
30	2	68	30	3758	0.66	4251.5	2313	358.6	0.209	3.03	7.78	71.9	37.22
30	2	68	40	3805	0.67	4324.1	2355	367.4	0.208	3.10	7.96	73.1	38.26

the packing density, which contract the glass network. Therefore, the structure of the glass will be strengthened and hence the increase of the rigidity will contribute to the increase in the ultrasonic velocity.

In solid materials, the Debye temperature (θ_D) plays an important role in the determination of elastic moduli and atomic vibrations. θ_D represents the temperature at which all the low frequency 'lattice' vibrational modes are excited (RAO, 2002). As a consequence, the Debye temperature, θ_D, which depends directly on the mean ultrasonic velocity and on the atomic vibrations of the lighter structural groups like phosphates will increase as the MoO₃ content increases. The increase in θ_D can be explained by taking into account two factors. Firstly, the clear shift of the vibrational modes in the IR absorption spectra towards higher frequencies as the MoO₃ content increases and the change in the relative strength of bonds in the glass network. The bond strength of Li_2O, Al_2O_3, P_2O_5 and MoO_3 are 77.9, 119.2, 28.2 and $69.8 \times 10^9 \, \mathrm{J \, m^{-3}}$ (LIDE, 2004). The increase of the bond strength, the rigidity and the average cross-link density of the studied glasses decrease the Poisson's ratio.

The values of the bulk modulus (K_e) and Young's modulus (Y) are listed in Table 1. As discussed before, addition of MoO₃ to the Li_2O-Al_2O_3-P_2O_5 glass creates new linkages attached to the phosphate structural units. These linkages have a high bond energy and increase both the number of bonds per unit glass formula unit and the packing density of the glass structure. On the other hand, the bulk modulus of a covalent network is determined by the bond density (number of bonds in a unit volume), and by the stretching force constant. The stretching force constant is related to the cation field strength of the modifier, i.e. high field strength cations polarize their environment strongly and enhance the ion-dipole interaction. Thus, the increase in the packing density can be attributed to two factors, firstly, the change in the coordination polyhedra of MoO₃ from MoO₆ to MoO₄, which in its turn change the type of bonding of the investigated glasses and secondly, the local contrac-

tion of the network around the Mo and Li cations that have a high-field-strength which polarizes their environment strongly and enhances the ion-dipole interactions. However, the elastic moduli are sensitive in a greater extent to the density of covalent bonds in the structure, which resist deformation. Therefore, it can be concluded that the elastic moduli will increase and these conclusions are in agreement with that reported earlier (DAMODARAN, 1989; SIDKEY, 2002; MUÑOZ *et al.*, 2004; SADDEEK *et al.*, 2009).

4. Conclusion

The analysis of IR spectra indicates that the Mo^{3+} ions are preferentially incorporated into the phosphate network as former forming the $[MoO_4]^{2-}$ units. New bonds have a high bond strength and bridging oxygens were created. The sound velocities, Debye temperature, and the elastic properties show an increasing trend with the increase in the MoO₃ content. This behavior was attributed to the increase of the cross link density; the number of network bonds per unit volume, the rigidity as well as the high-field-strength of Mo^{3+} polarizes their environment strongly.

Further work is required to study the electrical and optical properties of these materials with and without the radiation effect to improve the use in optoelectronic devices.

Acknowledgments

References

1. Abid M., Elmoudane M., Et-tabirou M. (2002), *Spectroscopic studies of the structure of sodium lead oligophosphate glasses*, Phys. Chem. Glasses, **43**, 267–270.

2. Bih L., Abbas L., Nadiri A., Khemakhem H., Elouadi B. (2008), *Investigations of molybdenum redox phenomenon in $Li_2O–MoO_3–P_2O_5$ phosphate glasses*, J. Mol. Struct. **872**, 1–9.

3. Boudlich D., Bih L., El Hassane Archidi M., Haddad M., Yacoubi A., Nadiri A., Elouadi B. (2002), *Infrared, Raman, and Electron Spin Resonance Studies of Vitreous Alkaline Tungsten Phosphates and Related Glasses*, J. Am. Ceram. Soc., **85**, 623–630.

4. Bridge B., Patel N. (1986), *The elastic constants and structure of the vitreous system Mo-P-O*, J. Mater. Sci., **21**, 1187–1205.

5. Bridge B., Patel N. (1987), *Composition dependence of the infra-red absorption spectra of molybdenum phosphate glasses and some crystalline analogues*, J. Non-Cryst. Solids, **91**, 27–42.

6. Brow R., Click C., Alam T. (2000), *Modifier coordination and phosphate glass networks*, J. Non-Cryst. Solids, **274**, 9–16.

7. Brow R. (2000), *Review: the structure of simple phosphate glasses*, J. Non-Cryst. Solids, **263**, 1–28.

8. Campbell J., Suratwala T. (2000), *Nd-doped phosphate glasses for high-energy/high-peak-power lasers*, J. Non-Cryst. Solids, **263**, 318–341.

9. Chowdari B., Gopalakrishnan R., Tang S., Kuok M. (1988), *Characterization of $Ag_2O:MoO_3:P_2O_5$ glasses*, Solid State Ion., **28**, 704–709.

10. Chowdari B., Tan K., Chia W., Gopalakrishnan R. (1991), *Thermal, physical, electrical and XPS studies of the $Li_2O: P_2O_5: MoO$ glass system*, J. Non-Cryst. Solids, **128**, 18–29.

11. Ciceo Lucacel R., Hulpus A., Simon V., Ardelean I. (2009), *Structural characterization of phosphate glasses doped with silver*, J. Non-Cryst. Solids, **355**, 425–429.

12. Cozar O., Magdas D., Ardelean I. (2008), *EPR study of molybdenum-lead-phosphate glasses*, J. Non-Cryst. Solids, **354**, 1032–1035.

13. Cozar O., Magdas D., Nasdala L., Ardelean I., Damian G. (2006), *Raman spectroscopic study of some lead phosphate glasses with tungsten ions*, J. Non-Cryst. Solids, **352**, 3121–3125.

14. Dai S., Sugiyama A., Hu L., Liu Z., Huang G., Jiang Z. (2002), *The spectrum and laser properties of ytterbium doped phosphate glass at low temperature*, J. Non-Cryst. Solids, **311**, 138–144.

15. Damodaran K., Rao K. (1989), *Elastic Properties of Alkali Phosphomolybdate Glasses*, J. Am. Ceram. Soc., **72**, 533–539.

16. Donald I. (1989), *Methods for improving the mechanical properties of oxide glasses*, J. Mater. Sci., **24**, 4177–4208.

17. ElBatal H., Hamdy Y., Marzouk S. (2008), *Gamma ray interactions with V_2O_5-doped sodium phosphate glasses*, Mater. Chem. Phys., **112**, 991–1000.

18. Eraiah B., Smitha M., Anavekar R. (2010), *Elastic properties of lead-phosphate glasses doped with samarium trioxide*, J. Phys. Chem. Solids, **71**, 153–155.

19. Higazy A., Bridge B. (1985), *Elastic constants and structure of the vitreous system Co_3O_4-P_2O_5*, J. Non-Cryst. Solids, **72**, 81-108.

20. Hudgens J., Brow R., Tallant D., Martin S. (1998), *Raman spectroscopy study of the structure of lithium and sodium ultraphosphate glasses*, J. Non-Cryst. Solids, **223**, 21-31.

21. Ivascu C., Timar Gabor A., Cozar O., Daraban L., Ardelean I. (2011), *FT-IR, Raman and thermoluminescence investigation of $P_2O_5–BaO–Li_2O$ glass system*, J. Molec. Struct., **993**, 249–253.

22. Jastrzebski W., Sitarz M., Bułat K. (2011), *Infrared spectroscopy of different phosphates structures Spectrochim*, Acta A, **79**, 722–727.

23. Jiang S., Myers M., Peyghambarian N. (1998), *Er^{3+} doped phosphate glasses and lasers*, J. Non-Cryst. Solids, **239**, 143–148.

24. Khafagy A. (2001), *Infrared and Ultrasonic Investigations of Some $[(MnO_2)_x–(P_2O_5)_{100−x}].1 wt\% Nd_2O_3$ Glasses*, Phys. Stat. Sol. (a), **186**, 105–114.

25. Lazarev A. (1968), *Kolebatielnyje spektry i strojenije silikatov* [in Russian], Nauka, Leningrad.

26. Lide D. (2004), *CRC Handbook of Chemistry and Physics*, 84th edition, CRC Press, Boca Raton, Fl.

27. Little Flower G., Sahaya Baskaran G., Srinivasa Reddy M., Veeraiah N. (2007), *The structural investigations of $PbO–P_2O_5–Sb_2O_3$ glasses with MoO_3 as additive by means of dielectric, spectroscopic and magnetic studies*, Physica B, **393**, 61–72.

28. Magdas D., Cozar O., Chis V., Ardelean I., Vedeanu N. (2008), *The structural dual role of Fe_2O_3 in some lead-phosphate glasses*, Vib. Spectrosc., **48**, 251–254.

29. Manupriya K., Thind K., Singh G., Sharma, Rajendran V. (2009), *Influence of addition of Al_2O_3 on physical, structural, acoustical and in-vitro bioactive properties of phosphate glasses*, Phys. Status Solidi A, **206**, 1447–1455.

30. Montenero A., Aielli M., Gnappi G., Lorenzi A., Sglavo V., Royer Carfagni G. (2004), *Mechanical properties of $PbO–ZnO–P_2O_5$ glasses*, Phys. Chem. Glasses, **46**, 538–543.

31. Moustafa Y., El-Egili K. (1998), *Infrared spectra of sodium phosphate glasses*, J. Non-Cryst. Solids, **240**, 144–153.

32. Muńoz F., Agulló-Rueda F., Montagne L., Marchand R., Durán A., Pascual L. (2004), *Structure and properties of $(25-x/2)Li_2O.(25-x/2)Na_2O. xPbO.50P_2O_5$ metaphosphate glasses*, J. Non-Cryst. Solids, **347**, 153–158.

33. Prasad S., Sahaya Baskaran G., Veeraiah N. (2005), *Spectroscopic, magnetic and dielectric investigations of BaO–Ga₂O₃–P₂O₅ glasses doped by Cu ions*, Phys. Stat. Sol.(a), **202**, 2812–2828.

34. Proulx P., Cormier G., Capobianco J., Champagnon B., Bettinelli M. (1994), *Raman and low frequency Raman spectroscopy of lead, zinc and barium metaphosphate glasses doped with Eu³⁺ ions*, J. Phys. Condens. Matter, **6**, 275–283.

35. Rao K. (2002), *Structural Chemistry of Glasses*, Elsevier, North Holland.

36. Reis S., Faria D., Martinelli J., Pontuschka W., Day D., Partiti C. (2002), *Structural features of lead iron phosphate glasses*, J. Non-Cryst. Solids, **304**, 188–194.

37. Saddeek Y. (2011), *Network structure of molybdenum lead phosphate glasses: Infrared spectra and constants of elasticity*, Physica B, **406**, 562–566.

38. Saddeek Y., Afifi H., Abd El-Aal N. (2007), *Interpretation of mechanical properties and structure of TeO₂–Li₂O–B₂O₃ glasses*, Physica B, **398**, 1–7.

39. Saddeek Y., Gaafar M., Bashier S. (2010), *Structural influence of PbO by means of FTIR and acoustics on calcium alumino-borosilicate glass system*, J. Non-Cryst. Solids, **356**, 1089–1095.

40. Saddeek Y., Shaaban E., Aly A., Sayed I. (2009), *Characterization of some lead vanadate glasses*, J. Alloys and Compounds, **478**, 447–452.

41. Selvaraj U., Rao K. (1985), *Characterization Studies of Molybdophosphate Glasses and a Model of Structural Defects*, J. Non-Cryst. Solids, **72**, 315–334.

42. Sharaf El-Deen L., Al Salhi M., Elkholy M. (2008), *Spectral properties of PbO–P2O5 glasses*, J. Non-Cryst. Solids, **354**, 3762–3766.

43. Sidkey M., El Mallawany R., Abousehly A., Saddeek Y. (2002), *Relaxation of longitudinal ultrasonic waves in some tellurite glasses*, Mater. Chem. Phys., **74**, 222–229.

44. Šubčik J., Koudelka L., Mošner P., Montagne L., Revel B., Gregora I. (2009), *Structure and properties of MoO₃-containing zinc borophosphate glasses*, J. Non-Cryst. Solids, **355**, 970–975.

45. Sudarsan V., Mishra R., Kulshreshth S. (2004), *Thermal and structural studies on TeO₂ substituted (PbO)₀.₅(P₂O₅)₀.₅ glasses*, J. Non-Cryst. Solids, **342**, 160–165.

46. Wells A. (1975), *Structural Inorganic Chemistry*, 4th edition, Clarendon Press, Oxford.